

Full-Dimensional Rate Enhancement for UAV-Enabled Communications via Intelligent Omni-Surface

Yifan Liu, *Student Member, IEEE*, Bin Duo, *Member, IEEE*, Qingqing Wu, *Senior Member, IEEE*, Xiaojun Yuan, *Senior Member, IEEE*, and Yonghui Li, *Fellow, IEEE*

Abstract

This paper investigates the achievable rate maximization problem of a downlink unmanned aerial vehicle (UAV)-enabled communication system aided by an intelligent omni-surface (IOS). Different from the state-of-the-art reconfigurable intelligent surface (RIS) that only reflects incident signals, the IOS can simultaneously reflect and transmit the signals, thereby providing full-dimensional rate enhancement. We formulate this rate maximization problem by jointly optimizing the IOS's phase shift and the UAV trajectory. Although it is difficult to solve it optimally due to its non-convexity, we propose an efficient algorithm to obtain a high-quality suboptimal solution. Simulation results show that the IOS-assisted UAV communications can achieve significant improvement in achievable rates compared to other benchmark schemes.

Index Terms

UAV communications, intelligent omni-surface, trajectory design, phase shift design.

Yifan Liu and Bin Duo are with Chengdu University of Technology, Chengdu, China (e-mail: liuyifan@stu.cdut.edu.cn; duobin@cdut.edu.cn). Qingqing Wu is with the State Key Laboratory of Internet of Things for Smart City, University of Macau, Macau, China (email: qingqingwu@um.edu.mo). Xiaojun Yuan is with the National Laboratory of Science and Technology on Communications, University of Electronic Science and Technology of China, Chengdu, China (e-mail: xjyuan@uestc.edu.cn). Yonghui Li is with the School of Electrical and Information Engineering, University of Sydney, NSW, Australia (yonghui.li@sydney.edu.au).

I. INTRODUCTION

With the commercialization of the fifth-generation (5G) wireless networks, the sixth generation (6G) wireless communication technology has recently attracted increasing attention by industry and academia [1]. **The reconfigurable intelligent surface (RIS), as an effective solution to overcome non-line-of-sight (NLoS) transmission and coverage blind spots, can significantly improve the spectral efficiency, energy efficiency, security, and reliability of communication systems [2].** Thus, the RIS has become a promising technology for the future 6G networks. In general, the RIS is an artificial surface made of electromagnetic material and consists of a large number of square metal patches, each of which can be digitally controlled to induce different reflection amplitudes and phases on incident signals [3]. By optimizing the RIS's phase shifts, the signals from different transmission paths can be aligned at the desired receiver to boost achievable rates [4].

On the other hand, due to line-of-sight (LoS) transmission and flexible mobility, unmanned aerial vehicles (UAVs) have gained widespread attention and have been applied in many applications [5]–[7]. Thanks to the low-profile and lightweight of RISs, they can be installed at proper locations to reconfigure propagation environments of air-to-ground channels, thus significantly enhancing communication quality. As shown in [8] and [9], the average achievable (secrecy) rates of RIS-assisted UAV communications can be significantly increased by jointly optimizing the UAV trajectory and the RIS's phase shifts. To provide better quality-of-service (QoS) for ground nodes that locate far apart, a UAV relaying system with the aid of a RIS was proposed in [10], where the relaying UAV forwards the received signals reflected from the RIS via intelligent phase alignment. The advantages of employing multiple RISs for enhancing the received power of the UAV-enabled communications were further investigated in [11]. Generally, the RIS can be placed on the outer surface of a building. In this case, the RIS can only reflect incident signals towards ground nodes. When the ground nodes are located indoors or in the back side of the RIS, their achievable rates may not benefit from the deployment of the RIS.

To address the above issue, the intelligent omni-surface (IOS) has been proposed as an upgrade of the RIS to realize the dual functionality of signal reflection and transmission [12]. Similar to the RIS, the IOS is made of multiple passive scattering elements and programmable PIN diodes, which can be appropriately designed and configured to customize the propagation environment [13]. Specifically, to realize full coverage of ground users, the IOS-assisted system was considered in [13], where the spectral efficiency is increased significantly by optimizing the phase shifts of the IOS. In [14], multiple indoor users obtain omni-directionally services from a small base station (SBS) with the aid of an IOS. By jointly optimizing the IOS analog beamforming and the SBS digital beamforming, the received power of multiple users is enhanced. Due to the advantages of the IOS for both reflection and transmission, it is essential to investigate whether the application of the IOS to the UAV communication system could provide higher achievable rates for ground nodes in all directions.

Motivated by the above, this paper considers a typical application scenario for UAV-enabled communications in 6G networks, where the UAV as an aerial base station (BS) provides communication services to a ground node. To achieve omni-directional rate enhancement, an IOS is installed to intelligently reflect/transmit incident signals from the UAV. We aim to maximize the average achievable rate by jointly optimizing the UAV trajectory and the

phase shift design of the IOS. To resolve the non-convexity of the formulated problem, we develop an efficient algorithm to obtain a suboptimal solution. Simulation results show that significantly higher achievable rates can be obtained by replacing the RIS with the IOS in the UAV-enabled communication system. Note that we are the first to introduce the IOS to the UAV communication system for providing the full-dimensional rate enhancement. Furthermore, due to the complex physical characteristics and the radiation pattern of the IOS, both the formulated objective function and our proposed algorithm are different from those in the conventional the RIS-aided UAV communication system [8]-[11].

II. SYSTEM MODEL AND PROBLEM FORMULATION

In this paper, we consider a typical application scenario for UAV-enabled communications, where a UAV flies on a mission to provide communication services to a ground node¹ (G). Owing to intelligent reflection as well as transmission of arrived signals, an IOS is deployed to enhance G's achievable rate in all directions. We characterize the position of the UAV, the IOS, and G via the three-dimensional Cartesian coordinate system. As such, it is assumed that the UAV flies at a fixed altitude z_U to communicate with G, whose location is denoted by $\mathbf{w}_G = [x_G, y_G]$, over a duration T . For convenience, T is divided into N time slots that are equal in length, i.e. $T = N\delta_t$, where δ_t is the length of each time slot. Thus, the horizontal trajectory of the UAV can be approximated by the discrete waypoints $\mathbf{q}[n] = [x[n], y[n]]$, $n \in \mathcal{N} = \{1, \dots, N\}$. We assume that both the UAV and G are equipped with a single omni-directional antenna. For the IOS with M elements [13], we denote by $\mathbf{w}_m = [x_m, y_m]$, $m \in \mathcal{M} = \{1, \dots, M\}$ and z_m the horizontal and vertical coordinates of the m th element of the IOS, respectively. Thus, the normalized power radiation patterns of the arrival signal and the departure signal of the IOS can be expressed as [13]

$$K_m^A[n] = |\cos^3 \theta_m^A[n]| = \left| \left(\frac{x[n] - x_m}{d_{U,m}[n]} \right)^3 \right|, \theta_m^A[n] \in (0, 2\pi), \quad (1)$$

$$K_m^D = \begin{cases} |\cos^3 \theta_m^D| = \left| \left(\frac{x_G - x_m}{d_{m,G}} \right)^3 \right|, \theta_m^D \in (0, \frac{\pi}{2}), \\ \epsilon |\cos^3 (\pi - \theta_m^D)| = \epsilon \left| \left(\frac{x_G - x_m}{d_{m,G}} \right)^3 \right|, \theta_m^D \in (\frac{\pi}{2}, 2\pi), \end{cases} \quad (2)$$

where $\theta_m^A[n]$ is the angle of arrival (AoA) of the signal from the UAV to m th element of the IOS in the n th time slot, θ_m^D is the angle of departure (AoD) of the signal from the m th element to G, ϵ is a constant that is determined by the hardware structure of the IOS [15], $d_{U,m}[n] = \sqrt{\|\mathbf{q}[n] - \mathbf{w}_m\|^2 + (z_U - z_m)^2}$ and $d_{m,G} = \sqrt{\|\mathbf{w}_G - \mathbf{w}_m\|^2 + z_m^2}$ are the distances from the m th element of the IOS to the UAV and to G, respectively. Thus, the reflective or transmissive power gain from the m th element of the IOS to G is given by [16]

$$g_m[n] = \sqrt{G_m K_m^A[n] K_m^D \delta_x \delta_y |\gamma_m|^2} \exp(-j\psi_m[n]), \quad (3)$$

¹Due to the space limitation, we consider the single ground node scenario. However, it can be readily extended to the case with multiple ground nodes by optimizing the communication scheduling for multiple ground nodes, while without changing the phase shift design of the IOS and the trajectory design of the UAV.

where G_m is the antenna power gain of the m th reconfigurable unit, δ_y and δ_z are the size of each element along Y and Z axes, respectively, $|\gamma_m|^2$ is the power ratio between the power of the signal reflected/transmitted by the IOS and the power of the incident signal, and $\psi_m[n]$ denotes the phase shift of the m th element in time slot n .

In this system, the UAV communicates with G via two links: the direct path from the UAV to G and the reflective-transmissive path from the UAV to G via the IOS. It is assumed that the channel coefficients from the UAV to G follow a practical Rician channel model, i.e.,

$$h_D[n] = \sqrt{\frac{\kappa}{1+\kappa}} h_D^{\text{LoS}}[n] + \sqrt{\frac{1}{1+\kappa}} h_D^{\text{NLoS}}[n], \quad (4)$$

where κ is the Rician factor. Furthermore, $h_D^{\text{LoS}}[n] = \sqrt{G^{tx} G^{rx} d_{U,G}^{-\alpha}} \exp\left(-j\frac{2\pi}{\lambda} d_{U,G}[n]\right)$ is the deterministic LoS component, where G^{tx} is the transmission antenna gain of the UAV antenna, G^{rx} is the receiving antenna gain of G, $d_{U,G}[n] = \sqrt{\|\mathbf{q}[n] - \mathbf{w}_G\|^2 + z_U^2}$ is the distance from the UAV to G, and α is the path-loss exponent. The NLoS component is defined as $h_D^{\text{NLoS}}[n] = \sqrt{G^{tx} G^{rx} d_{U,G}^{-\alpha}} h_{SS}$, where $h_{SS} \sim \mathcal{CN}(0, 1)$ is the small-scale fading component modeled by a circularly symmetric complex Gaussian (CSCG) random variable. Similarly, the channel coefficients from the UAV to G via the m th IOS element can also be formulated as a Rician channel, which is given by

$$h_m[n] = \sqrt{\frac{\kappa}{1+\kappa}} h_m^{\text{LoS}}[n] + \sqrt{\frac{1}{1+\kappa}} h_m^{\text{NLoS}}[n]. \quad (5)$$

The LoS component of $h_m[n]$ can be expressed as

$$\begin{aligned} h_m^{\text{LoS}}[n] &= \frac{\lambda \sqrt{G^{tx} K_m^A[n] G^{rx} K_m^D} \exp\left(\frac{-j2\pi(d_{U,m}[n] + d_{m,G})}{\lambda}\right)}{(4\pi)^{\frac{3}{2}} d_{UAV,m}[n] d_{m,MU}} \times g_m[n] \\ &= \frac{\lambda K_m^A[n] K_m^D \sqrt{G^m G^{tx} G^{rx} \delta_z \delta_y |\gamma_m|^2}}{(4\pi)^{\frac{3}{2}} d_{U,m}[n] d_{m,G}} \times \exp\left(\frac{-j2\pi(d_{U,m}[n] + d_{m,G} + \psi_m[n])}{\lambda}\right), \end{aligned} \quad (6)$$

where λ is the carrier wavelength. The NLoS component of $h_m[n]$ can be represented as

$$h_m^{\text{NLoS}}[n] = \frac{\lambda K_m^A[n] K_m^D \sqrt{G^m G^{tx} G^{rx} \delta_z \delta_y |\gamma_m|^2}}{(4\pi)^{\frac{3}{2}} d_{U,m}[n] d_{m,G}} h_{SS}. \quad (7)$$

Therefore, the channel coefficient from the UAV to G via the IOS in the n th time slot can be given by

$$h[n] = \sum_{m=1}^M h_m[n] + h_D[n]. \quad (8)$$

It is assumed that the UAV transmits with its maximum power denoted by P . Then, the average achievable rate in bits/second/Hertz (bps/Hz) at G in the n th time slot is given by

$$\bar{R} = \frac{1}{N} \sum_{n=1}^N \log_2 \left(1 + \eta |h[n]|^2 \right), \quad (9)$$

where $\eta = \frac{P}{\sigma^2}$, and σ^2 is the additive white Gaussian noise power at the corresponding receiver.

Our goal is to maximize the average achievable rate by jointly optimizing the horizontal UAV trajectory $\mathbf{Q} \triangleq \{\mathbf{q}[n], n \in \mathcal{N}\}$ and the IOS's phase shift $\Psi \triangleq \{\psi_m[n], n \in \mathcal{N}, m \in \mathcal{M}\}$ over the entire N time slots. Therefore, the optimization problem can be expressed as

$$\max_{\mathbf{Q}, \Psi} \bar{R} \quad (10a)$$

$$\text{s.t. } \|\mathbf{q}[n] - \mathbf{q}[n-1]\|^2 \leq D^2, \forall n, \quad (10b)$$

$$\mathbf{q}[N] = \mathbf{q}_F, \mathbf{q}[1] = \mathbf{q}_0, \quad (10c)$$

$$0 \leq \psi_m[n] \leq 2\pi, \forall n, m, \quad (10d)$$

where \mathbf{q}_0 and \mathbf{q}_F denote the initial and final horizontal positions of the UAV, respectively, $D = v_{max}\delta_t$ is the maximum distance that the UAV can move horizontally within a time slot, and v_{max} is the maximum airspeed of the UAV. Problem (10) is difficult to solve because it is a complicated non-linear fractional programming problem with an objective function that is not jointly concave with respect to its coupled optimization variables. In the following section, we will propose an alternating optimization algorithm to solve problem (10).

III. PROPOSED ALGORITHM

In this section, we propose an alternating optimization algorithm to solve problem (10) by alternately optimizing the IOS's phase shift Ψ and the UAV trajectory \mathbf{Q} until the convergence of the algorithm.

A. IOS Phase Shift Design

With any feasible UAV trajectory \mathbf{Q} , the optimization problem of phase-shift Ψ can be expressed as

$$\max_{\Psi} |h[n]|^2 \quad (11)$$

$$\text{s.t. (10d).}$$

Optimized Ψ allows the signals from different paths to be combined coherently at G, thereby maximizing its average achievable rate. Since $h_m^{\text{NLoS}}[n]$ and $h_D^{\text{NLoS}}[n]$ are both constants and both nonnegative, maximizing $|h[n]|^2$ is to maximize $|\sum_{m=1}^M h_m^{\text{LoS}}[n] + h_D^{\text{LoS}}[n]|^2$. Thus, problem (17) can be equivalently converted into the following optimization problem:

$$\max_{\Psi} \left| \sum_{m=1}^M h_m^{\text{LoS}}[n] + h_D^{\text{LoS}}[n] \right|^2 \quad (12)$$

$$\text{s.t. (10d).}$$

Proposition 1: The optimal phase shift for the m th element of the IOS is

$$\psi_m[n] = \frac{2\pi}{\lambda} (d_{UAV,G}[n] - d_{UAV,m}[n] - d_{m,G}). \quad (13)$$

Proof: See Appendix A. ■

B. UAV Trajectory Optimization

With the optimal phase shift obtained by (13), the UAV trajectory optimization problem can be expressed as

$$\max_{\mathbf{Q}} \frac{1}{N} \sum_{n=1}^N \log_2 \left(1 + \eta \zeta^2[n] \left| \sqrt{\frac{\kappa}{1+\kappa}} e^{-j d_{U,G}[n]} \lambda + \sqrt{\frac{1}{1+\kappa}} h_{SS} \right|^2 \right) \quad (14)$$

s.t. (10b)-(10c),

where $\zeta[n] = \sum_{m=1}^M \frac{J_m \beta_m |x[n] - x_m|^3}{d_{UAV,m}^4[n]} + \frac{K}{d_{UAV,G}^{\alpha/2}[n]}$, $J_m = \frac{\lambda \sqrt{G^{tx} G^{rx} G_m \delta_z \delta_y |\gamma_m|^2}}{(4\pi)^{\frac{3}{2}}}$, $K = \sqrt{G^{tx} G^{rx}}$ and $\beta_m = \frac{K_m^D}{d_{m,G}}$. It is observed that problem (14) is still non-convex with respect to \mathbf{Q} . To solve this problem, we have the following proposition to convert this problem into an equivalent problem.

Proposition 2. Problem (14) is equivalent to the following problem:

$$\max_{\mathbf{Q}, \mathbf{s}, \mathbf{u}, \mathbf{v}} \frac{1}{N} \sum_{n=1}^N \log_2 \left(1 + \eta \left(\sum_{m=1}^M J_m \beta_m \frac{e^{s[n]}}{e^{u_m[n]}} + K e^{v[n]} \right)^2 \right) \quad (15a)$$

$$\text{s.t. } e^{s[n]} \leq |x[n]|^3, \quad (15b)$$

$$e^{u_m[n]} \geq d_{U,m}^4[n], \quad (15c)$$

$$e^{v[n]} \leq d_{U,G}^{-\alpha/2}[n], \quad (15d)$$

(10b)-(10c).

where $\mathbf{s} = \{s[n]\}_{n=1}^N$, $\mathbf{u} = \{u_m[n]\}_{n=1}^N \{m=1}^M$, and $\mathbf{v} = \{v[n]\}_{n=1}^N$. *Proof:* See Appendix B. \blacksquare

Note that, after the variable replacement, the objective function (15a) is transformed to a log-sum-exp function which is convex [17]. However, constraints (15b)-(15d) are still non-convex. Since the first-order Taylor approximation of a convex function is a global underestimator, it can be applied at any local points $s^{(l)}[n]$, $u_m^{(l)}[n]$, $v^{(l)}[n]$ and $|x^{(l)}[n]|$ in the l th iteration for (15a)-(15d) i.e.,

$$\log_2 \left(1 + \eta \left(\sum_{m=1}^M J_m \beta_m \frac{e^{s[n]}}{e^{u_m[n]}} + K e^{v[n]} \right)^2 \right) \geq \log_2 A^{(l)}[n] + \frac{B^{(l)}[n]}{A^{(l)}[n] \ln 2} (s[n] - s^{(l)}[n]) + \sum_{m=1}^M \frac{C_m^{(l)}[n]}{A^{(l)}[n] \ln 2} (u_m[n] - u_m^{(l)}[n]) + \frac{D^{(l)}[n]}{A^{(l)}[n] \ln 2} (v[n] - v^{(l)}[n]), \quad (16)$$

$$|x^{(l)}[n]|^3 + \frac{3x^{(l)}[n]^3}{|x^{(l)}[n]|} (x[n] - x^{(l)}[n]) \geq e^{s[n]}, \quad (17)$$

$$e^{\frac{u_m^{(l)}[n]}{2}} + \frac{e^{\frac{u_m^{(l)}[n]}{2}}}{2} (u_m[n] - u_m^{(l)}[n]) \geq d_{U,m}^2[n], \quad (18)$$

$$e^{\frac{-4v^{(l)}[n]}{\alpha}} - \frac{4e^{\frac{-4v^{(l)}[n]}{\alpha}}}{\alpha} (v[n] - v^{(l)}[n]) \geq d_{U,G}^2[n], \quad (19)$$

where

$$A^{(l)}[n] = 1 + \eta \left(\left(\sum_{m=1}^M J_m \beta_m \frac{e^{s^{(l)}[n]}}{e^{u_m^{(l)}[n]}} \right)^2 + K^2 e^{2v^{(l)}[n]} + 2K \sum_{m=1}^M J_m \beta_m \frac{e^{s^{(l)}[n] + v^{(l)}[n]}}{e^{u_m^{(l)}[n]}} \right),$$

$$B^{(l)}[n] = \eta \left(2 \left(\sum_{m=1}^M J_m \beta_m \frac{e^{s^{(l)}[n]}}{e^{u_m^{(l)}[n]}} \right)^2 + 2K \sum_{m=1}^M J_m \beta_m \frac{e^{s^{(l)}[n] + v^{(l)}[n]}}{e^{u_m^{(l)}[n]}} \right),$$

$$C_m^{(l)}[n] = \eta \left(-2 \left(\sum_{m=1}^M J_m \beta_m \frac{e^{s^{(l)}[n]}}{e^{u_m^{(l)}[n]}} \right) J_m \beta_m \frac{e^{s^{(l)}[n]}}{e^{u_m^{(l)}[n]}} - 2J_m K \beta_m \frac{e^{s^{(l)}[n]+v^{(l)}[n]}}{e^{u_m^{(l)}[n]}} \right),$$

$$D^{(l)}[n] = \eta \left(2K^2 e^{2v^{(l)}[n]} + 2K \sum_{m=1}^M J_m \beta_m \frac{e^{s^{(l)}[n]+v^{(l)}[n]}}{e^{u_m^{(l)}[n]}} \right). \text{ With (16)-(19), problem (15) can be approximated as}$$

$$\max_{\mathbf{Q}, \mathbf{s}, \mathbf{u}, \mathbf{v}} \frac{1}{N} \sum_{n=1}^N \frac{B^{(l)}[n]}{A^{(l)}[n] \ln 2} s[n] + \sum_{m=1}^M \frac{C_m^{(l)}[n]}{A^{(l)}[n] \ln 2} u_m[n] + \frac{D^{(l)}[n]}{A^{(l)}[n] \ln 2} v[n], \quad (20)$$

s.t. (10a)-(10b), (17)-(19).

Problem (20) is now a convex optimization problem and can therefore be efficiently solved by a standard CVX solver [18].

C. Overall Algorithm

By using our proposed algorithm, problem (10) can be efficiently solved by alternately optimizing variables Ψ and \mathbf{Q} , while its solution converges to a preset accuracy μ . Since the two subproblems are solved by applying CVX via the standard interior point method, their computational complexity can be obtained as $O((MN)^{3.5} \log(1/\mu))$ and $O((4N + MN)^{3.5} \log(1/\mu))$, respectively. Besides, the computational complexity of the alternating optimization is $O(\log(1/\mu))$. Thus, the total computational complexity of our proposed algorithm is in the order of $O((4N + MN)^{3.5} \log^2(1/\mu))$.

IV. SIMULATION RESULTS

In this section, we evaluate the performance of the IOS-assisted UAV-enabled communications based on the proposed algorithm (denoted by IA scheme) and compare it with the following benchmark solutions: 1) RIS-assisted UAV communications (denoted by RA scheme) proposed in [8], where the IOS in our proposed system is replaced by an RIS; 2) IOS-assisted UAV communications with the fixed trajectory (denoted by IA-FT scheme), where the UAV takes off from \mathbf{q}_0 to G at v_{max} , then hovers above G as long as possible, and finally flies towards \mathbf{q}_F at v_{max} by the end of T ; 3) Conventional UAV communication (denoted by CUC scheme) without the aid of IOS or RIS. We assume that the IOS and G are located at (0, 0, 40) m and (-100, -20, 0) m, respectively. Other simulation parameters are set as: $\mathbf{q}_0 = [-400, 20]$ m, $\mathbf{q}_F = [400, 20]$ m, $v_{max} = 25$ m/s, $\mu = 0.0001$, $G_{tx} = G_{rx} = 1$, $\delta_t = 1$ s, $\kappa = 3$, $P = 0.1$ W, $\alpha = 5$, $\sigma^2 = -80$ dBm, $\lambda = 0.05$ m, $\gamma_m = 1$, $\epsilon = 3.55$ [15].

Fig. 1(a) presents the different trajectories of the UAV by various algorithms with $T = 150$ s and $M = 6000$. Comparing to the RA scheme that the UAV only hovers at the location on the left side of the RIS, the UAV in the IA scheme hovers close to both sides of the IOS to gain the benefit of omni-directional rate enhancement. The reason behind this observation is that the IOS is not only able to reflect the arrived signal from the UAV like the RIS, but also to transmit the signal. This results in higher rate compared to the RA scheme, which can be verified in the following Fig. 1(b). Fig. 1(b) illustrates the average achievable rates by different schemes with $M = 6000$ versus T . It is observed that the average achievable rates are significantly improved with the increase of T , since the UAV can fly to more favorable hovering locations to transmit more information. Particularly, the RA scheme achieves a significant rate gain over the CUC scheme, which confirms that the proper deployment of the RIS can

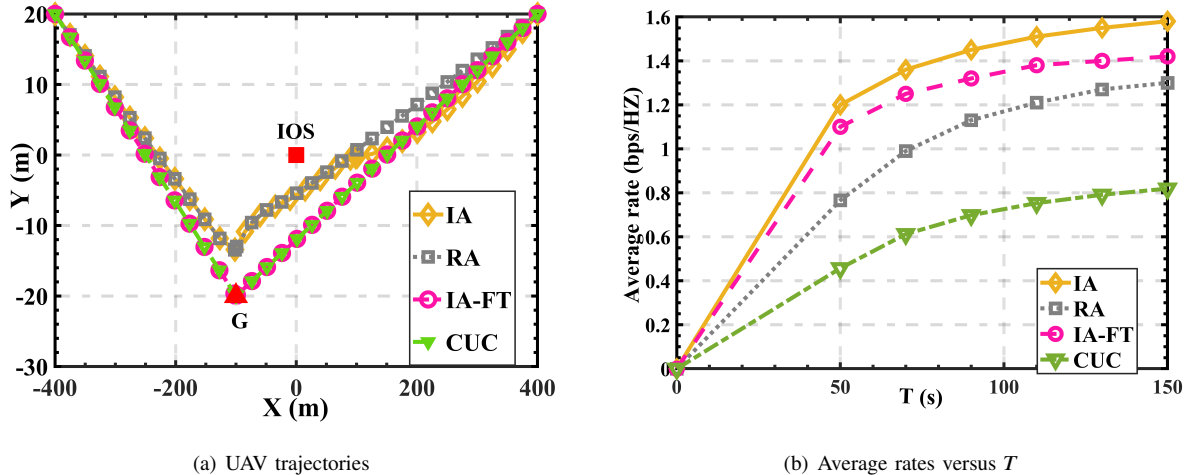


Fig. 1: UAV Trajectories and average achievable rates by different schemes.

indeed enhance the achievable rate of the system effectively. Our proposed IA scheme obtains more significant rate improvement compared to the RA scheme. This indicates that properly designing the UAV trajectory and the IOS's phase shift can benefit from the flexible mobility of the UAV as well as the full-dimensional rate enhancement with the assistance of the IOS, thus unlocking the full potential of IOS-aided UAV communications. Fig. 2(a) shows the

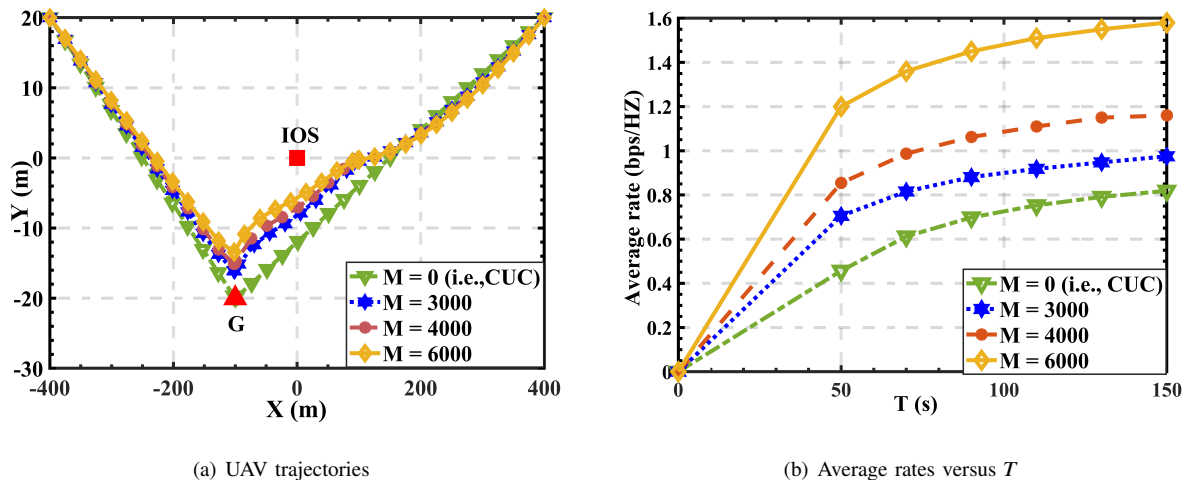


Fig. 2: UAV Trajectories and average achievable rates by different M .

different UAV trajectories by our proposed IA scheme versus M for $T = 150$ s. Note that with the increase of M , the UAV's trajectory and its hovering locations tend to approach the IOS due to the greater benefit that the IOS can provide from its both sides, which can be verified in Fig. 2(b). Fig. 2(b) shows the average achievable rates for different M versus T . As expected, the rate performance is improved significantly when equipping with more elements in the IOS due to the larger passive beamforming gain.

V. CONCLUSION

In this paper, we investigated the potential for increasing the rate performance by leveraging the novel reflective-transmissive IOS. The objective is to maximize the average achievable rate. We proposed an efficient algorithm to obtain a suboptimal solution by alternately optimizing the IOS's phase shift and the UAV trajectory. Simulation results have shown that the IOS-aided scheme achieves noteworthy gain as compared to the conventional UAV-enabled communications with/without the aid of a traditional RIS. This demonstrates the potential for using the IOS to provide the full coverage of communication services in future 6G networks.

APPENDIX A

PROOF OF PROPOSITION 1

To maximize $|h[n]|$ shown in problem (12), the triangle inequality can be applied, i.e.,

$$\begin{aligned} \left| \sum_{m=1}^M h_m^{\text{LoS}}[n] + h_D^{\text{LoS}}[n] \right| &\stackrel{a}{\leq} \sum_{m=1}^M \left| h_m^{\text{LoS}}[n] \right| + \left| h_D^{\text{LoS}}[n] \right| = \sum_{m=1}^M \left| \frac{J_m \beta_m |x[n] - x_m|^3}{d_{U,m}^4[n]} \exp\left(\frac{-j2\pi(d_{U,m}[n] + d_{m,G}[n])}{\lambda} - j\psi_m[n]\right) \right| \\ &+ \left| \frac{K}{d_{U,G}^{\alpha/2}[n]} \exp\left(\frac{-j2\pi d_{U,G}[n]}{\lambda}\right) \right|, \end{aligned} \quad (21)$$

where $J_m = \frac{\lambda \sqrt{G^{\text{tx}} G^{\text{rx}} G_m \delta_z \delta_y |\gamma_m|^2}}{(4\pi)^{\frac{3}{2}}}$, $K = \sqrt{G^{\text{tx}} G^{\text{rx}}}$ and $\beta_m = \frac{K_m^D}{d_{m,G}}$. Note that (a) holds with equality if and only if $\psi_m[n] + \frac{2\pi(d_{U,m}[n] + d_{m,G})}{\lambda} = \frac{2\pi(d_{U,G}[n])}{\lambda}$ [19]. Therefore, the optimal solution to problem (12) is

$$\psi_m[n] = \frac{2\pi}{\lambda} (d_{U,G}[n] - d_{U,m}[n] - d_{m,G}). \quad (22)$$

APPENDIX B

PROOF OF PROPOSITION 2

To solve problem (14), we first apply Euler's formula to calculate $|h[n]|^2$ as below

$$\begin{aligned} |h[n]|^2 &= \zeta[n]^2 \left| \sqrt{\frac{\kappa}{1+\kappa}} \exp\left(\frac{-jd_{U,G}[n]}{\lambda}\right) + \sqrt{\frac{1}{1+\kappa}} h_{SS} \right|^2 \\ &= \zeta[n]^2 \left(\left| \sqrt{\frac{\kappa}{1+\kappa}} \cos\left(\frac{-jd_{U,G}[n]}{\lambda}\right) + \sqrt{\frac{1}{1+\kappa}} \text{Re}(h_{SS}) \right|^2 \right. \\ &\quad \left. + |j|^2 \left| \sqrt{\frac{\kappa}{1+\kappa}} \sin\left(\frac{-jd_{U,G}[n]}{\lambda}\right) + \sqrt{\frac{1}{1+\kappa}} \text{Im}(h_{SS}) \right|^2 \right) \\ &= \frac{\zeta[n]^2}{1+\kappa} \left(\kappa + |h_{SS}|^2 + 2\sqrt{\kappa} \text{Re}(h_{SS}) \cos\left(\frac{d_{U,G}[n]}{\lambda}\right) \right. \\ &\quad \left. - 2\sqrt{\kappa} \text{Im}(h_{SS}) \sin\left(\frac{d_{U,G}[n]}{\lambda}\right) \right), \end{aligned} \quad (23)$$

where $\zeta[n] = \sum_{m=1}^M \frac{J_m |x[n] - x_m|^3}{d_{U,m}^4[n]} \frac{|x_G - x_m|^3}{d_{m,G}^4} + \frac{K}{d_{U,G}^{\alpha/2}[n]}$. Therefore, the channel power gain from the UAV to G via IOS can be expressed as

$$\mathbb{E}(|h[n]|^2) = \sum_{m=1}^M \frac{J_m |x[n] - x_m|^3}{d_{UAV,m}^4[n]} \frac{|x_G - x_m|^3}{d_{m,G}^4} + \frac{K}{d_{UAV,G}^{\alpha/2}[n]}, \quad (24)$$

where $\mathbb{E}(\cdot)$ is the expectation operator. With (24), problem (10) can be transformed to

$$\max_{\mathbf{Q}} \frac{1}{N} \sum_{n=1}^N \log_2 \left(1 + \eta \left(\sum_{m=1}^M \frac{J_m \beta_m |x[n]|^3}{d_{U,m}^4[n]} + \frac{K}{d_{U,G}^{\alpha/2}[n]} \right)^2 \right) \quad (25)$$

s.t. (10b)-(10c).

To solve this non-convex problem, we further introduce the variables $e^s[n]$, $e^{u_m}[n]$ and $e^v[n]$ to replace $|x[n]|^3$, $d_{U,m}^4[n]$ and $d_{U,G}^4[n]$, respectively. Then, we have problem (15) which completes the proof.

REFERENCES

- [1] S. Chen, Y.-C. Liang, S. Sun, S. Kang, W. Cheng, and M. Peng, "Vision, requirements, and technology trend of 6G: How to tackle the challenges of system coverage, capacity, user data-rate and movement speed," *IEEE Wireless Communications*, vol. 27, no. 2, pp. 218–228, 2020.
- [2] Q. Wu, S. Zhang, B. Zheng, C. You, and R. Zhang, "Intelligent reflecting surface-aided wireless communications: A tutorial," *IEEE Trans. Commun.*, vol. 69, no. 5, pp. 3313–3351, 2021.
- [3] Q. Wu and R. Zhang, "Towards smart and reconfigurable environment: Intelligent reflecting surface aided wireless network," *IEEE Commun. Mag.*, vol. 58, no. 1, pp. 106–112, 2020.
- [4] Q. Wu and R. Zhang, "Intelligent reflecting surface enhanced wireless network via joint active and passive beamforming," *IEEE Trans. Wireless Commun.*, vol. 18, no. 11, pp. 5394–5409, 2019.
- [5] S. Zhang, H. Zhang, and L. Song, "Beyond D2D: Full dimension UAV-to-Everything communications in 6G," *IEEE Trans. Veh. Technol.*, vol. 69, no. 6, pp. 6592–6602, 2020.
- [6] Y. Zeng, Q. Wu, and R. Zhang, "Accessing from the sky: A tutorial on UAV communications for 5G and beyond," *Proc. IEEE*, vol. 107, no. 12, pp. 2327–2375, 2019.
- [7] B. Duo, Q. Wu, X. Yuan, and R. Zhang, "Energy efficiency maximization for full-duplex UAV secrecy communication," *IEEE Trans. Veh. Technol.*, vol. 69, no. 4, pp. 4590–4595, 2020.
- [8] S. Li, B. Duo, X. Yuan, Y.-C. Liang, and M. Di Renzo, "Reconfigurable intelligent surface assisted UAV communication: Joint trajectory design and passive beamforming," *IEEE Wireless Commun. Lett.*, vol. 9, no. 5, pp. 716–720, 2020.
- [9] S. Li, B. Duo, M. Di Renzo, M. Tao, and X. Yuan, "Robust secure UAV communications with the aid of reconfigurable intelligent surfaces," *IEEE Trans. Wireless Commun.*, pp. 1–1, 2021.
- [10] L. Yang, F. Meng, J. Zhang, M. O. Hasna, and M. D. Renzo, "On the performance of RIS-assisted dual-hop UAV communication systems," *IEEE Trans. Veh. Technol.*, vol. 69, no. 9, pp. 10385–10390, 2020.
- [11] L. Ge, P. Dong, H. Zhang, J.-B. Wang, and X. You, "Joint beamforming and trajectory optimization for intelligent reflecting surfaces-assisted UAV communications," *IEEE Access*, vol. 8, pp. 78702–78712, 2020.
- [12] N. DOCOMO. "DOCOMO conducts worlds first successful trial of transparent dynamic metasurface". Jan. 2020. [Online]. Available: <https://www.nttdocomo.co.jp/english/info/mediacenter/pr/2020/011700.html>
- [13] S. Zhang, H. Zhang, B. Di, Y. Tan, Z. Han, and L. Song, "Beyond intelligent reflecting surfaces: Reflective-transmissive metasurface aided communications for full-dimensional coverage extension," *IEEE Trans. Veh. Technol.*, vol. 69, no. 11, pp. 13905–13909, 2020.
- [14] S. Zhang *et al.*, "Intelligent omni-surface: Ubiquitous wireless transmission by reflective-transmissive metasurface." [Online]. Available: <https://arxiv.org/abs/2011.00765>
- [15] C. Pfeiffer and A. Grbic, "Metamaterial Huygens' surfaces: Tailoring wave fronts with reflectionless sheets," *Phys. Rev. Lett.*, vol. 110, no. 19, p. 197401, 2013.

- [16] W. Tang *et al.*, “Wireless communications with reconfigurable intelligent surface: Path loss modeling and experimental measurement,” *IEEE Trans. Wireless Commun.*, vol. 20, no. 1, pp. 421–439, 2021.
- [17] S. Boyd and L. Vandenberghe, *Convex Optimization*, Cambridge, U.K.: Cambridge Univ. Press, 2004.
- [18] B. S. Grant, M. CVX: Matlab Software for Disciplined Convex Programming, Version 2.2. (2020). [Online]. Available: <http://cvxr.com/cvx>
- [19] M. Hua, L. Yang, Q. Wu, C. Pan, C. Li, and A. Lee Swindlehurst, “UAV-assisted intelligent reflecting surface symbiotic radio system,” *IEEE Trans. Wireless Commun.*, pp. 1–1, 2021.